The American Journal of Pathology, Vol. 191, No. 12, December 2021

The American Journal of
PATHOLOGY
ajp.amjpathol.org

VASCULAR BIOLOGY, ATHEROSCLEROSIS, AND ENDOTHELIUM BIOLOGY

B Cell—Activating Factor Antagonism Attenuates the Growth of Experimental Abdominal Aortic Aneurysm

Michael D. Spinosa,* William G. Montgomery,* Melissa Lempicki,† Prasad Srikakulapu,‡ Matthew J. Johnsrude,† Coleen A. McNamara,‡ Gilbert R. Upchurch, Jr,* Gorav Ailawadi,* Norbert Leitinger,§ and Akshaya K. Meher†§

From the Departments of Surgery and Pharmacology,§ and the Robert M. Berne Cardiovascular Research Center,‡ University of Virginia, Charlottesville, Virginia; and the Department of Microbiology and Immunology,† East Carolina University, Greenville, North Carolina*

Accepted for publication August 20, 2021.

Address correspondence to Akshaya K. Meher, Ph.D., Department of Microbiology and Immunology, Brody School of Medicine, East Carolina University, 600 Moye Blvd., Greenville, NC 27834. E-mail: mehera19@ecu.edu.

B cell—activating factor (BAFF), part of a tumor necrosis factor family of cytokines, was recently identified as a regulator of atherosclerosis; however, its role in aortic aneurysm has not been determined. Here, the study examined the effect of selective BAFF antagonism using an anti-BAFF antibody (blocks binding of BAFF to receptors BAFF receptor 3, transmembrane activator and CAML interactor, and B-cell maturation antigen) and mBaffR-mFc (blocks binding of BAFF to BAFF receptor 3) on a murine model of abdominal aortic aneurysm (AAA). In a prevention strategy, the antagonists were injected before the induction of AAA, and in an intervention strategy, the antagonists were injected after the induction of AAA. Both strategies attenuated the formation of AAA. In the intervention group, BAFF antagonism depleted most of the mature B-cell subsets in spleen and circulation, leading to enhanced resolution of inflammation in AAA as indicated by decreased infiltration of B cells and proinflammatory macrophages and a reduced number of apoptotic cells. In AAA tissues, B cells and macrophages were found in close contact. *In vitro*, B cells, irrespective of treatment with BAFF, impaired the efferocytosis activity of macrophages, suggesting a direct innate role of B cells on macrophage function. Altogether, BAFF antagonism affects survival of the mature B cells, promotes resolution of inflammation in the aorta, and attenuates the growth of AAA in mice. *(Am J Pathol 2021, 191: 2231—2244; https://doi.org/10.1016/j.ajpath.2021.08.012)*

Abdominal aortic aneurysm (AAA) is characterized by enlargement of the abdominal aorta. According to the Centers for Disease Control and Prevention, in 2018, 9923 deaths were caused by aortic aneurysm. Men aged >65 years are more prone to developing AAA. Mortality rates for ruptured AAA repair remain as high as 48% and have not improved substantially.[1] Thus far, the only treatment available for AAA is repair via surgery. Evidently, there is a great need to elucidate the mechanisms of AAA growth to develop noninvasive treatment options.

During AAA formation, degradation of aortic fibers and vascular smooth muscle layer weaken the aortic wall.[2–4] Infiltration of leukocytes has been reported both in human and experimental murine AAAs.[5–8] A study on AAA specimens collected from humans revealed 41% of infiltrated mononuclear cells are B cells.[5] In murine experimental AAAs, both B1 and B2 B cells infiltrate the aorta, with B2 cells comprising 90% of B cells.[7] Although B cells constitute only 4% to 5% of the aortic infiltrated cells, depletion of total B cells using a rituximab mimetic anti-CD20 antibody (Ab) attenuates aortic infiltration of macrophages, reduces aortic inflammation, retains aortic structure, and protects mice from AAA.[7,8] However, how B cells promote aortic inflammation and AAA formation is unknown.

Supported by NIH National Heart, Lung, and Blood Institute (NHLBI) grants R01 HL146685 (A.K.M.), R01 HL126668 (G.A.), and R01 HL124131 (G.R.U.); American Heart Association grant 14SDG20380044 (A.K.M.); a University of Virginia LaunchPad for Diabetes Innovation Grant (A.K.M.); funds from East Carolina University (A.K.M.); and NIH National Institute of Diabetes and Digestive and Kidney Diseases grant R01 DK096076 (N.L.).

Disclosures: A.K.M. has published patent application PCT/US2019/029348, entitled "Composition and methods for treating abdominal aortic aneurysm." No embargo restriction is associated with this patent.

https://doi.org/10.1016/j.ajpath.2021.08.012

B cell–activating factor (BAFF, BLyS, or TALL-1), a member of the tumor necrosis factor family of cytokines, is a critical survival factor for mature B cells.[9] Apart from providing the survival signal, BAFF promotes differentiation of B cells, Ab class switching, and Ab secretion.[10] Interestingly, secreted BAFF can adopt a 3-mer or a 60-mer configuration.[11] The 3-mer preferentially binds to the BAFF receptor 3 (BR3), whereas the 60-mer can bind to all three of the BAFF receptors: BR3, transmembrane activator and CAML interactor (TACI), and B-cell maturation antigen (BCMA).[12,13] BAFF and the receptor BR3 are critical for the differentiation of transitional 1 B cells to transitional 2 and other mature B-cell subsets, which are together considered as B2 cells. Although BAFF receptors are expressed in many cell types, antagonism of BAFF or blocking BR3 primarily depleted B2 B cells, sparing $CD4^+$, $CD8^+$, natural killer, and regulatory T cells in mice.[14,15] In murine models of atherosclerosis, genetic deficiency or blocking BR3 leads to a significant decrease in the number of proatherogenic B2 B cells; it also retains natural IgM-producing atheroprotective B1a B cells, decreases in the tissue deposition of IgGs, increases in the deposition of IgM in the aorta, decreases in inflammation, and protects mice from atherosclerosis.[16,17] Furthermore, anti-BAFF Ab treatment or genetic deficiency of BAFF has B2 cell–depleting, B1a cell–sparing activity that protects mice from metabolic diseases.[18,19] Here, BAFF antagonists were used to determine whether depleting B2 cells in wild-type (WT) mice affects aneurysm formation using a topical elastase model of AAA.

In this study, the two BAFF antagonists used were: a murine monoclonal anti-BAFF Ab that blocks binding of BAFF to BR3, TACI, and BCMA[14]; and mBaffR-mFc, a murine BR3 ecto-domain fused to murine IgG1 Fc fragment that blocks binding of BAFF to BR3. Administration of either of the antagonists in a prevention strategy and in an intervention strategy attenuated the growth of experimental AAA in mice. The antagonists not only depleted the B2 cells but also depleted B1 cells in spleen and blood and attenuated aortic inflammation, with a significant decrease in the infiltration of macrophages and B cells. However, in the time frame of this study, the level of plasma immunoglobulins was partly reduced, and the ratio of deposition of IgG to IgM in AAAs of antagonist-treated and control mice was similar. Whereas the BAFF antagonist-mediated protection from AAA would be caused primarily by depletion of mature B cells, this study identified a novel innate role of B cells that is involved in clearance of apoptotic cells by macrophages. Therefore, an innate role of B cells in the growth of murine experimental AAAs is proposed.

Materials and Methods

Human Tissue Collection

Collection of human aortic tissue from patients undergoing open AAA repair was approved by the University of Virginia Institutional Review Board for Health Sciences Research (institutional review board no. 17042), and written consents were obtained from all patients before inclusion in the study. The tissues collected were immediately fixed in formalin, embedded in paraffin, and 5 μm cross-sections cut for immunohistochemistry. The investigation conforms to the principles outlined in the Declaration of Helsinki for the use of human tissues and subjects. Alternative to the collected human tissues, slides containing 5 μm cross-sections of human AAA tissues were obtained from OriGene (Rockville, MD). The selection of tissue cross-section for immunohistology was based on the presence of clinical signs of AAA such as aortic degradation and cellular infiltrates.

Mice

Seven-week–old male C57BL/6 mice (catalog number 000664, WT) and the BAFF knockout mice (B6.129S2-Tnfsf13btm1Msc/J, catalog number 010572) were obtained from The Jackson Laboratory (Bar Harbor, ME). Genotype of the BAFF knockout mouse was confirmed by using the genotyping protocol provided by The Jackson Laboratory. All mice were given water and normal mouse diet (Prolab IsoPro RMH 3000 5P76, LabDiet, St. Louis, MO), except for the mice undergoing AAA surgery, which were given a minimal phytoestrogen diet (2016 Teklad Diet; Harlan Laboratories, Indianapolis, IN) *ad libitum*. For the AAA induction studies, 8- to 9-week–old mice were used; for the B-cell and bone marrow isolation, 8- to 12-week–old mice were used. All protocols were approved by East Carolina University and University of Virginia Animal Care and Use Committee.

Murine Experimental AAA

Male C57BL/6 (WT) mice were used for the induction of AAA via a topical elastase model. Various anti-BAFF reagents injected in the mice were the control Ab (IgG1κ, Bio X Cell, Lebanon, NH; catalog number BE0083), anti-BAFF Ab (IgG1κ, AdipoGen Life Sciences, San Diego, CA; catalog number AG-20B-0063PF), or mBaffR-mFc (Biogen, Cambridge, MA). In the prevention strategy, the mice were injected with 1 or 2 mg/kg of anti-BAFF, 2 mg/kg of mBaffR-mFc Ab, or 1 or 2 mg/kg of a control Ab. After 14 days, the mice were injected again with the Abs, and AAA was induced via a topical elastase model. AAA formation was determined 14 days after the AAA induction. In the intervention strategy, the anti-BAFF, mBaffR-mFc, or the control Ab was injected 7 days after the induction of AAA, and AAA formation was determined after 7 days.

The methods for induction of anesthesia (isoflurane inhalation), surgical procedure for murine AAA formation via topical elastase method, and postoperative analgesia (buprenorphine sustained release) have been previously described.[20] Briefly, after the abdominal aorta is circumferentially dissected from approximately 2 mm below the left renal vein to the bifurcation, a fine tip pipette is then

used for topical application of 5 μL of elastase (MilliporeSigma, Burlington, MA; 10.1 mg protein/mL, 19 U/mg protein) to the exposed aortic adventitia for 5 minutes. After 5 minutes, the aorta is dried with a cotton tip applicator, the intestines are returned to the abdominal cavity, and the laparotomy is closed in layers. Aneurysm formation was examined 14 days after the surgery.

Mice from each group were euthanized under anesthesia by overdose and exsanguination. The abdominal aorta, from below the left renal vein to the bifurcation, was dissected. The external aortic adventitia diameter was measured at its maximum diameter and at the intact self-control portion just below the left renal vein by using video microscopy with NIS-Elements D.3.10 software attached to the microscope (Nikon SMX-800; Nikon, Melville, NY). Aortic dilation percentage was determined by the following: (maximal AAA diameter − self-control aortic diameter)/maximal AAA diameter × 100%. A dilation ≥100% was considered to be positive for AAA.[20] On postoperative day 14, after diameter measurement, blood, spleen, and aneurysm tissues were collected for analyses. Two surgeons performed the surgeries (M.D.S. and W.G.M.), and during the surgery and the aortic size determination, the surgeons were blinded to various treatments. No mice were observed to be sick, and hence no mice were excluded in the study. AAA phenotypes of all mice are presented as dot plots in the figures.

Quantification of Immunoglobulins in Plasma

The IgG1, IgG2b, IgG2c, IgA, and IgM immunoglobulins were quantified from mouse plasma using Ig Isotyping Mouse Instant ELISA Kit (Thermo Fisher Scientific, Waltham, MA; catalog number 88-50660-22).

Immunohistochemistry of AAA Cross-Sections

Five micrometer aortic cross-sections were hydrated with a series of solvents, which were HistoChoice Clearing Agent (MilliporeSigma), 100% ethanol, 90% ethanol, 70% ethanol, 20% ethanol, and then water. After 15 minutes of treatment with hydrogen peroxide, antigen retrieval was performed by boiling the slides in the Antigen Unmasking Solution (Vector Laboratories, Burlingame, CA; H-3300). After antigen retrieval, the aortic sections were treated with Avidin/Biotin blocking kit (Vector Laboratories) and 10% donkey serum and incubated with primary Ab for 14 to 16 hours at 4°C. Primary Abs were detected by biotinylated donkey secondary Abs, VECTASTAIN Elite ABC Kit (Vector Laboratories, PK-6100) and ImmPACT DAB Peroxidase (HRP) Substrate (Vector Laboratories, SK-4105). The DAB Peroxidase Substrate develops brown color. Some of the cross-sections were stained with hematoxylin to identify nuclei. For multi-color staining, after DAB staining, the slides were treated with the second primary Ab and identified in a similar method as the first primary Ab; however, the biotinylated secondary Abs were reacted with alkaline phosphatase streptavidin (Vector Laboratories, SA-5100) and Vector Blue substrate (Vector Laboratories, SK-5300), which develops a blue color. The slides were mounted with an aqueous mounting medium before image acquisition on a Laxco LMI 6000 Series Inverted microscope (Fisher Scientific). The primary Abs used are: anti-CD20 Ab (Santa Cruz Biotechnology, Dallas, TX; catalog number sc-7735, 1:200, Normal Goat IgG isotype control), BAFF (Abcam, Cambridge, MA; catalog number ab16081, 1:100, Normal Rat IgG isotype control), CD79a (Abcam, catalog number ab79414, 1:100, Normal Rabbit IgG isotype control), BCMA (Abcam, catalog number ab199264, 1:500, Normal Rabbit IgG isotype control), BAFF-R (Abcam; catalog number ab5965, 1:1000, Normal Rabbit IgG isotype control), TACI (Abcam; catalog number ab79023, 1:500, Normal Rabbit IgG isotype control), IgG-biotin (LSBio, Seattle, WA; catalog number LS-C662993, 1:200, Normal Goat IgG isotype control), IgM-biotin (LSBio; catalog number LS-C662999, 1:200, Goat anti-Mouse IgM isotype control; LSBio; catalog number LS-C316493), smooth muscle actin (Novus Biologicals, Littleton, CO; catalog number NB600-531, 1:600, Normal Rabbit IgG isotype control), tumor necrosis factor-α (Novus Biologicals; catalog number NBP1-19532, 1:300, Normal Rabbit IgG isotype control), IL-1β (R&D Systems, Minneapolis, MN; catalog number AF-401-NA, 1:100, Normal Goat IgG isotype control), and inducible nitric oxide synthase (Thermo Fisher Scientific; catalog number PA3-030A, 1:1000, Normal Rabbit IgG isotype control). The isotype control Abs used are from R&D Systems: Normal Rabbit IgG Control (catalog number AB-105-C), Normal Goat IgG Control (catalog number AB-108-C), and Normal Rat IgG Control (catalog number 6-001-A).

Stained areas in the images were calculated by using ImageJ software version 1.53 (NIH, Bethesda, MD; *http://imagej.nih.gov/ij*). As a negative control, primary Abs were not added to one of the AAA sections on the same slide. Apoptotic cells were identified by using the TUNEL Assay Kit (HRP-DAB) from Abcam (catalog number ab206386) and counted manually under a microscope. Standard method for Verhoeff-Van Gieson staining was performed at the Cardiovascular Research Center histology core at the University of Virginia to stain the elastin layers. The images were acquired on an Inverted Laxco LMI 6000 Series Microscope, and area quantification was performed by using ImageJ software version 1.53c. Authors quantifying the images were blinded for the treatment strategy (M.L. and M.J.J.).

Flow Cytometry Quantification

After the collection of spleen and blood samples, the spleen was passed through a 70 μm pore size strainer, and red blood cells were lysed from both solenocytes and 100 μL of blood. The cells were blocked with purified anti-mouse CD16/32 (BioLegend, San Diego, CA; catalog number 101302, 1:100) and stained with the following fluorescent

conjugated Abs for 30 minutes on ice: PerCP-Cyanine5.5 anti-CD19 (BioLegend; catalog number 115534, 1:200), Alexa Fluor 488 anti-B220 (BioLegend; catalog number 103225, 1:50), APC-Cyanine7 anti-CD21 (BioLegend; catalog number 123418, 1:200), APC anti-CD23 (BioLegend; catalog number 101620, 1:100), Brilliant Violet 785 anti−major histocompatibility complex II (BioLegend; catalog number 107645, 1:100), Brilliant Violet 650 anti-IgD (BioLegend; catalog number 405721, 1:100), PE Cyanine7 anti-CD38 (BioLegend; catalog number 102718, 1:400), PE anti-IgM (BioLegend; catalog number 406508, 1:50), Alexa Fluor 488 Peanut Agglutinin (Thermo Fisher Scientific; L21409, 1:200), APC R700 anti-CD138 (BD Biosciences, Franklin Lakes, NJ; catalog number 565176, 1:50), PE Cyanine7 anti-CD3 (BioLegend; catalog number 100220, 1:50), PE Cyanine7 anti-F4/80 (eBioscience, San Diego, CA; catalog number 25-4801-82, 1:100), and PE anti−GL-7 (BioLegend; catalog number 144608, 1:100). Invitrogen DAPI (4',6-diamidino-2-phenylindole, dihydrochloride) (catalog number D1306) or LIVE/DEAD Fixable Violet Dead Cell Stain Kit (Thermo Fisher Scientific; catalog number L34955) was used for staining the dead cell. After the staining, CountBright Absolute Counting Beads (Molecular Probes, Eugene, OR; catalog number C36950) were added to the samples and were run on the flow cytometer machine LSRFortessa (equipped with laser lines 488 nm, 405 nm, 561 nm, and 640 nm or with 355 nm, 405 nm, 488 nm, and 640 nm; Becton Dickinson, Franklin Lakes, NJ). Fluorescent minus one controls were used for each Ab in the experiment. The gating strategy to identify the B-cell subpopulations is shown in Supplemental Figure S1 and described by Guo et al.[21] Data analysis and quantification were performed by using FlowJo version 10.6.2 (FlowJo LLC, Ashland, OR).

Murine B-Cell Isolation and Preparation of Bone Marrow−Derived Macrophages

Murine B cells were isolated by using the Pan B Cell Isolation Kit II (Miltenyi Biotec, Auburn, CA; catalog number 130-104-443) or the EasySep Mouse Pan-B Cell Isolation Kit (STEMCELL Technologies, Cambridge, MA; catalog number 19844) that labels the non−B cells with a cocktail of biotinylated CD4, CD11c, CD49b, CD90.2, Gr-1, and Ter-119 Abs and depletes from the splenocytes to provide highly pure B cells. After isolation, the B cells were suspended in complete RPMI medium (RPMI 1640 medium containing 10% heat inactivated fetal bovine serum, 1× antibiotic-antimycotic, 20 mmol/L HEPES Buffer solution, 1× GlutaMAX-I, 1 mmol/L sodium pyruvate, 1× MEM Non-Essential Amino Acids Solution, and 55 μmol/L 2-Mercaptoeathanol from Thermo Fisher Scientific). B-cell density was determined by using Countess II FL and counting chamber slides from Thermo Fisher Scientific. Purity of the B cells were found to be >96% as determined by cell surface expression of CD19 (PerCP-Cy5.5 anti-CD19) and B220 (Alexa Fluor 488 anti-B220) using flow cytometry.

For the preparation of bone marrow−derived macrophages, bone marrow cells from the femur and tibia of BAFF knockout mice were collected, red blood cells were lysed with lysis buffer (0.83% NH_4Cl, 0.084% $NaHCO_3$ and 1 mmol/L EDTA), and the cells were cultured at a density of 1 to 2 × 10^6 cells/mL in RPMI 1640 medium containing 10% heat inactivated fetal bovine serum, 1× antibiotic-antimycotic, and 20 mmol/L HEPES Buffer solution, supplemented with 10% granulocyte colony-stimulating factor containing culture supernatant (a gift from Prof. Mark D. Mannie, East Carolina University) or 20% L929 (NCTC clone 929; ATCC, Manassas, VA) culture supernatant. The culture medium was changed on the fourth day and then on every second day. On the eighth day, differentiation to macrophages was confirmed by surface expression of PE-Cyanine7 F4/80 and APC CD11b by flow cytometry.

Co-Culture of B Cells and Macrophages and the Engulfment Assay

To prepare the apoptotic thymocytes, thymocytes were isolated from a C57BL/6 mouse, red blood cells were lysed, and the cells were suspended in RPMI 1640 medium containing 1× antibiotic-antimycotic and cultured for 14 to 16 hours with 1 μmol/L dexamethasone. The cells were then washed with Hank's Balanced Salt Solution (Gibco Hanks' Balanced Salt Solution with Calcium Chloride and Magnesium Chloride), stained with CypHer5E NHS Ester (5 μmol/L; Cytiva, Marlborough, MA; catalog number PA15401), washed again, and suspended in complete medium. Apoptosis was confirmed by using the Annexin V Staining kit from Thermo Fisher Scientific (catalog number BDB556419) and flow cytometry. As an alternative to CypHer5E staining, apoptotic thymocytes were stained with DiI (V-22885; Molecular Probes) and then labeled with biotin by using the EZ-Link Sulfo-NHS-Biotin kit (A39256; Thermo Fisher Scientific).

Macrophages were stained with CellTracker Green CMFDA Dye (10 μmol/L; Thermo Fisher Scientific; catalog number C2925) and seeded at a density of 1 million cells per well on a flat 24-well nontreated tissue culture plate and polarized to M1 type by treating with lipopolysaccharide and interferon-γ for 16 hours as described previously[22] in complete RPMI medium. B cells isolated from mouse spleen were treated with 100 ng/mL of BAFF 3-mer, BAFF 60-mer, or left untreated for the 16 hours in complete RPMI medium. Both the B cells and macrophages were washed three times with the complete medium and co-cultured at a 1:1 ratio for the next 16 hours. Engulfment assays were initiated by addition of 5 million apoptotic thymocytes to the macrophage/B cells co-culture and subjected to incubation at 37°C for 1 hour. After incubation, the cells were washed with phosphate-buffered saline, trypsinized, and analyzed on a flow cytometer. Macrophages were identified by using

CellTracker Green fluorescence. Alternatively, engulfment assays were initiated by addition of 5 million DiI-stained and biotin-labeled apoptotic thymocytes to the unpolarized (M0) macrophage/B cells co-culture and subjected to incubation at 37°C for 30 minutes. After incubation, the cells were washed with phosphate-buffered saline, trypsinized, stained with Streptavidin Alexa Fluor 647 Conjugate (Molecular Probes; S32357, 1:500) for 15 minutes on ice, washed to remove unbound conjugates and analyzed on a flow cytometer. The macrophages were treated for 1 hour or 30 minutes with cytochalasin D (10 μmol/L;Cayman Chemicals, Ann Arbor, MI) before the addition of apoptotic thymocytes as a negative control for the engulfment assay.

Statistical Analysis

The data were analyzed by using GraphPad Prism 8 (GraphPad Software, La Jolla, CA) and Excel (Microsoft Corporation, Redmond, WA), and they are presented as means ± SEM or means ± SD. *In vitro* assays were performed in quadruplicate and repeated at least two times. Differences between mean values of two groups were determined by using *t*-tests. Means of multiple groups were compared by using one-way analysis of variance. The D'Agostino-Pearson normality test was performed on each group. If the *P* value was not significant (>0.05), a two-tailed parametric test was used; if the *P* value was significant (<0.05) or if the number of samples was four, a two-tailed nonparametric *t*-test (*U*-test) was used to determine significant differences between the groups. In the multiple comparisons, if a significant difference was found among the groups, pairs of groups were compared by using a parametric or nonparametric *t*-test. Statistical analyses are provided in each figure legend. Differences between the groups were considered significant when $P < 0.05$. *P* values >0.05 are indicated in the graphs.

Results

BAFF and BAFF Receptors Are Expressed in Human and Murine AAAs

To examine the possibility of BAFF signaling in B cells in AAA, whether B cells and BAFF are co-localized in AAA tissue was first determined. Serial cross-sections of human and murine AAAs were stained with B cell–specific Abs (anti-CD79α for human and anti-CD20 for mouse), anti-BAFF, anti-BR3, anti-TACI, and anti-BCMA Abs. In human AAAs, B-cell clusters and B cells expressing BR3, TACI, and BCMA were observed in the microenvironment of BAFF (Figure 1A). Experimental AAA was induced in mice via the topical elastase method, and AAAs were collected 14 days after AAA induction. Similar to human AAAs, B cells were localized in the microenvironment of BAFF in murine AAAs (Figure 1B). Furthermore, B cells in murine AAA tissue expressed BR3, TACI, and BCMA (Figure 1C). Altogether, these results suggest that B cells expressing BAFF receptor BR3 are localized in human and murine AAAs.

BAFF Antagonists Attenuate AAA Formation

Next, anti-BAFF Ab and mBaffR-mFc were used to determine whether BAFF or BAFF signaling via BR3 is critical for the growth of murine AAA using a topical elastase model.[20] In the prevention strategy, the mice were injected with 1 or 2 mg/kg of anti-BAFF, 2 mg/kg of mBaffR-mFc, or 1 or 2 mg/kg of a control Ab (the Ab dose was selected based on the first report of anti-BAFF Ab[14]). After 14 days, the mice were injected again with the BAFF antagonists, and AAA was induced; aneurysm formation was determined 14 days after the AAA induction. Compared with the control Ab–injected group of mice, AAA formation was significantly attenuated in the anti-BAFF group and the mBaffR-mFc group (1 mg/kg Ab, $n = 6$ to 7: control, 181.1 ± 7.3%; anti-BAFF, 144.6 ± 12%; 2 mg/kg Ab, $n = 5$ to 6: control, 174.7 ± 23.8%; anti-BAFF, 109.8 ± 4.4%; and 2 mg/kg, $n = 8$: control, 118.3 ± 8.7%; mBaffR-mFc, 63.6 ± 8.8%) (Figure 2, A and B), suggesting blocking the BAFF or BR3 binding site of BAFF before the induction of aneurysm attenuates AAA formation.

Using the topical elastase model of murine AAA, Spinosa et al[23] reported that 3 days after the induction of aneurysm, the aorta undergoes significant degradation with an increase in aortic inflammation. A significant increase in aortic size is also detected 7 days after aneurysm induction.[24] Therefore, in the intervention strategy, 7 days after the induction of AAA, the anti-BAFF, mBaffR-mFc, or the control Ab was injected, and aneurysm formation was determined after 7 days. AAA growth was strikingly attenuated in the anti-BAFF and the mBaffR-mFc groups (2 mg/kg, $n = 6$ per group: control, 159.3 ± 16.5%; anti-BAFF, 81.2 ± 4.3%; mBaffR-mFc, 95.1 ± 3.7%) (Figure 2C). These results show that BAFF binding to BR3 is critical for AAA growth.

BAFF Antagonists Significantly Deplete Mature B-Cell Subsets and Decrease Immunoglobulin Deposition in the Aorta

Genetic deficiency of BR3 in mice markedly depletes the B2-cell population, decrease infiltration of B cells to atherosclerotic lesions, decrease the levels of IgG1 and IgG2 in plasma, and inhibit the deposition of IgG1 and IgG2 in the lesions. However, the B1-cell population is preserved,[17] which protects mice from atherosclerosis by natural IgM.[25,26] Furthermore, germinal center–derived IgG Abs promote atherosclerosis,[27] whereas marginal zone B cells are atheroprotective.[28] Therefore, the effect of blocking BAFF on the dynamics of B-cell subsets (Supplemental Figure S1) in the spleen and blood was determined,

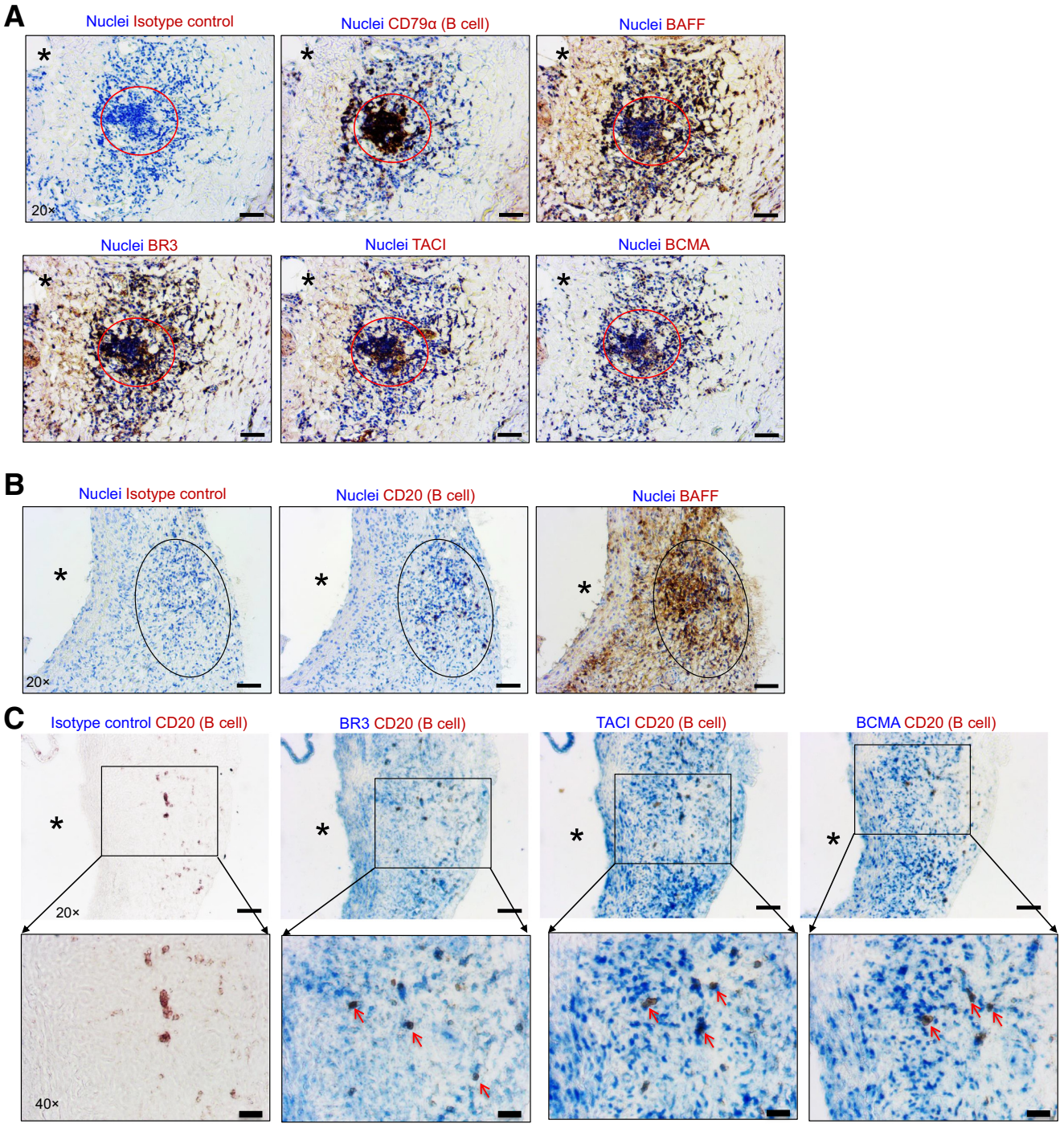

Figure 1 B cell–activating factor (BAFF) and BAFF receptors are expressed in human and murine abdominal aortic aneurysm (AAAs). **A:** Immunohistochemistry of aortic serial cross-sections showing images of B cells, BAFF, and BAFF receptors (brown) and nuclei (blue, hematoxylin) in human AAA. **Circles** indicate B cell–rich areas. **B:** Immunohistochemistry of aortic serial cross-sections showing images of B cells and BAFF (brown) and nuclei (blue, hematoxylin) in murine AAA. **Ovals** indicate B cell–rich areas. **C:** Immunohistochemistry of aortic serial cross-sections showing images of B cell (brown) or B cell (brown) and BAFF receptor (blue) staining in murine AAA. **Arrows** indicate co-localized staining of B cells and BAFF receptors, and **asterisks** indicate the direction of lumen or the lumen in all panels. Scale bars: 50 μm (**A**, **B**, and **C**, **top row**); 20 μm (**C**, **bottom row**). Original magnification: ×20 (**A, B**, and **C**, **top row**); ×40 (**C**, **bottom row**). BCMA, B-cell maturation antigen; BR3, BAFF receptor 3; TACI, transmembrane activator and CAML interactor.

plasma immunoglobulins were quantified, and deposition of immunoglobulins in the murine AAA tissues was examined.

Except for transitional 1B cells, total B2 cells (all the mature B-cell subtypes), including B1 cells, were depleted in the blood (not shown) and in the spleen after anti-BAFF or mBaffR-mFc injection in the prevention (Supplemental Figure S2) and in the intervention (Figure 3, A and B) groups. The number of germinal center and memory B cells

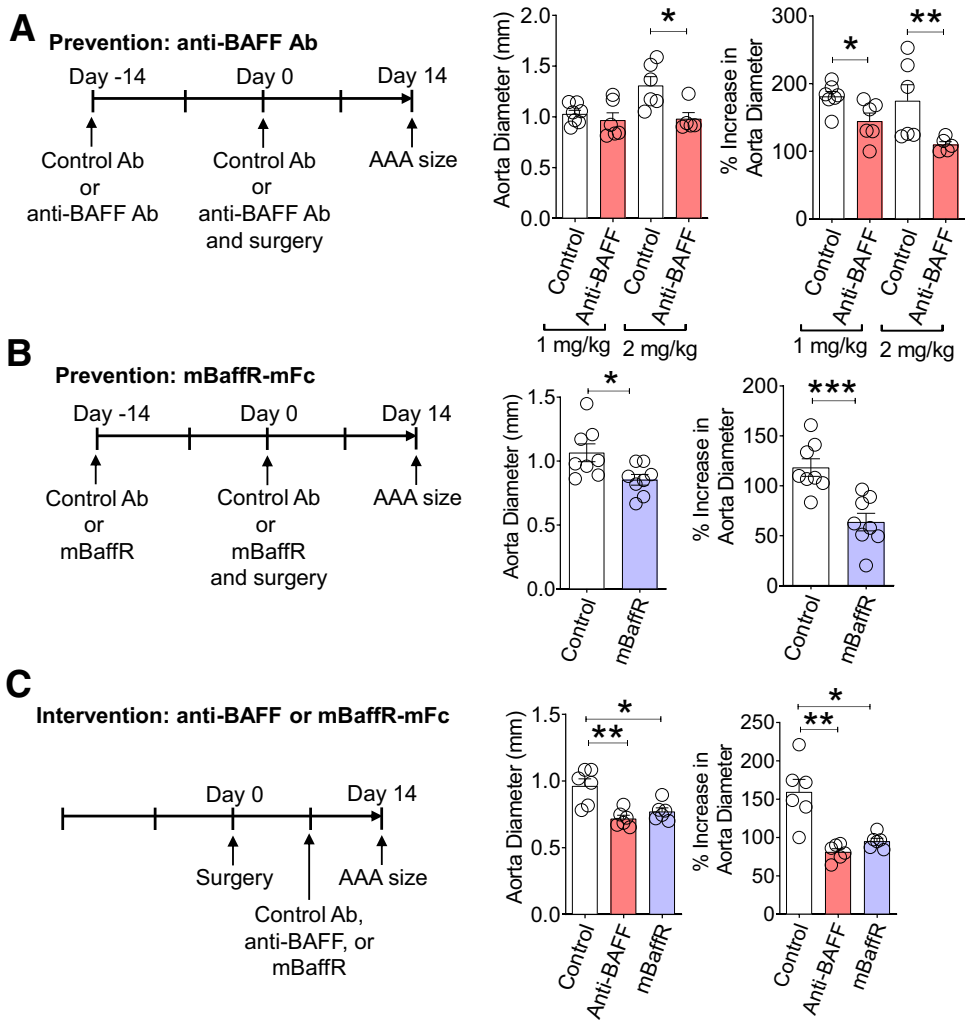

Figure 2 Pharmacologic inhibition of B cell–activating factor (BAFF) attenuates abdominal aortic aneurysm (AAA) growth. **A** and **B:** In the prevention strategy, wild-type mice were intravenously injected with 1 mg/kg or 2 mg/kg of anti-BAFF antibody (Ab), 2 mg/kg of mBaffR-mFc (murine BAFF receptor 3 ecto-domain fused to murine IgG1 Fc fragment that blocks binding of BAFF to BAFF receptor 3), or a control Ab once in 14 days. After 14 days of the Ab injection, AAA was induced via the topical elastase model. Aorta diameter (in millimeters) and increase in aorta diameter (%) compared with a proximal elastase untreated abdominal aortic segment was determined after 14 days of AAA induction. **C:** In the intervention strategy, AAA was induced in three groups of wild-type mice via the topical elastase model. Seven days after the induction, the mice were injected intravenously with 2 mg/kg control Ab, anti-BAFF, or mBaffR-mFc. Seven days after the Ab injection, aorta diameter (in millimeters) and increase in aorta diameter (%) were determined. Data are expressed as means ± SEMs. $n = 6$ to 7 (**A** and **B**, 1 mg/kg of anti-BAFF Ab); $n = 5$ to 6 (**A** and **B**, 2 mg/kg of anti-BAFF Ab); $n = 8$ (**A** and **B**, 2 mg/kg of mBaffR-mFc); $n = 6$ per group (**C**). $^{*}P < 0.05$, $^{**}P < 0.01$, and $^{***}P < 0.001$ (one-way analysis of variance followed by a parametric unpaired *t*-test).

tended to be lower in all the anti-BAFF– and mBaffR-mFc–injected groups. However, statistically significant changes were only noted in the mBaffR-mFc prevention group (Supplemental Figure S2). Further cellular analysis revealed significant decreases in the expression level of CD23 and major histocompatibility complex II[13] on the surface of $CD19^{+}$ B cells in spleen and blood of mice from the intervention groups (Figure 3C).

The levels of IgG1 and IgG2b in plasma were variably affected by anti-BAFF or mBaffR-mFc injections. In the prevention groups, the IgG2b levels were significantly reduced in the anti-BAFF Ab-injected mice but not in the mBaffR-mFc–injected mice (Supplemental Figure S3, A–C). Plasma IgM levels were not significantly affected in these groups. A significantly higher level of plasma IgG1 was detected in the control IgG1 Ab-injected mice than in the anti-BAFF– or mBaffR-mFc–injected intervention groups. In a separate experiment, the enzyme-linked immunosorbent assay kit used for the detection of the immunoglobulins identified the injected control IgG1 up to 14 days and hence found a high level of IgG1 in the control groups (Supplemental Figure S3D). In the intervention groups, the levels of plasma IgG2b and IgM were found to be marginally lower in the anti-BAFF and mBaffR-mFc groups compared with the control (Figure 4A). Altogether, these data suggest that the roles of germinal center and marginal zone B cells, or plasma IgG1 and IgG2, are not dominant ones in the pathogenesis of AAA in this murine model.

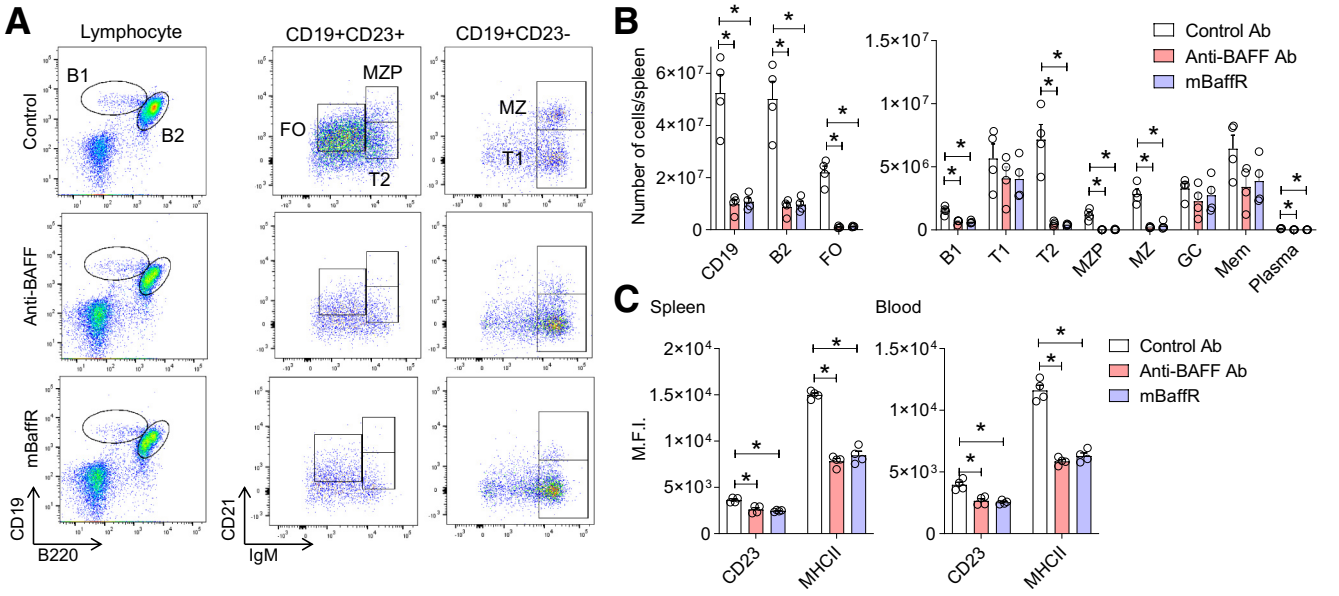

Figure 3 Anti—B-cell-activating factor (BAFF) or mBaffR-mFc (murine BAFF receptor 3 ecto-domain fused to murine IgG1 Fc fragment that blocks binding of BAFF to BAFF receptor 3) treatment significantly depleted mature B-cell subsets. **A:** Representative flow cytometry plots showing depletion of transitional 2 (T2), follicular (FO), marginal zone progenitor (MZP), and marginal zone (MZ) but not transitional 1 (T1) B cells in the spleens of mice from the intervention groups. **B:** Quantification of B-cell subsets in the spleens of mice from the intervention groups. **C:** Surface expression of CD23 and major histocompatibility complex II (MHCII) on $CD19^{+}$ B cells from the spleen and blood of mice from the intervention groups. Data are expressed as means ± SEMs (**B** and **C**). $n = 4$ (**B**); $n = 4$ mice per group (**C**). $^{*}P < 0.05$ (one-way analysis of variance followed by a nonparametric *U*-test). M.F.I., mean fluorescence intensity.

Next, the AAA tissues collected from the intervention group were examined for the deposition of IgG and IgM. The rationale for selecting the intervention group was the shorter duration of Ab treatment after the induction of AAA. The deposition of IgG was significantly lower, and IgM trended to lower, in the antagonist-treated groups (Figure 4B). However, no significant difference in ratio of deposition of IgG to IgM was found in the aortas of the control and the antagonist-treated mice, suggesting other mechanisms of AAA formation.

BAFF Antagonists Retain Aortic Structure and Attenuate Aortic Inflammation

Next, the aortic structure, infiltration of immune cells, and inflammation of AAA tissues from the intervention groups of mice were examined. As expected, total aortic size and adventitial layer were smaller, and the elastin fiber area was larger, in the anti-BAFF— and the mBaffR-mFc—treated mice compared with the control group (Figure 5A). Noticeable degradation of the elastin layer and the smooth muscle cell layer was identified in all groups (Figure 5, A and B). The infiltration of B cells was attenuated in the AAAs of the anti-BAFF— or mBaffR-mFc—treated mice (Figure 5C). Furthermore, infiltration of macrophages, as detected by the F4/80 marker, and the staining area of the proinflammatory cytokines inducible nitric oxide synthase, tumor necrosis factor-α, and IL-1β, which are primarily produced by macrophages (as indicated by overlapped staining areas in serial aortic cross-sections), were significantly lower in the anti-BAFF— and mBaffR-mFc—treated mice (Figure 5D). These results suggest that anti-BAFF and mBaffR-mFc treatment decreased aortic inflammation concomitant with attenuated aortic infiltration of B cells.

B Cells Skew Macrophage Engulfment Efficiency

Spleen is the primary source of circulating mature B cells; in the anti-BAFF and mBaffR-mFc intervention groups, except for the germinal center B cells, other mature B-cell subsets were depleted in the spleen. In addition, B cells did not accumulate in the aorta, and AAA growth was attenuated. This is similar to a previous report showing that depletion of B cells via anti-CD20 Ab protects mice from AAA.[8] However, whether BAFF-activated B cells modulate macrophage function to promote inflammation in AAA is unknown. Immunostaining the cross-sections of human and mouse AAAs indicated that B cells and macrophages were in direct contact (Figure 6A). One of the primary functions of macrophages at the site of inflammation is removal of apoptotic cells, impairment of which promotes inflammation. A significantly higher number of apoptotic cells were detected in the AAAs of the control Ab—treated mice compared with the anti-BAFF— or mBaffR-mFc—treated mice (Figure 6B). This result, together with quantification of proinflammatory markers (Figure 5D), quantification of B cells in AAA (Figure 5C), and localization of B cells in the BAFF microenvironment (Figure 1, A and B), suggest that BAFF-activated B cells in AAA impair phagocytic clearance by

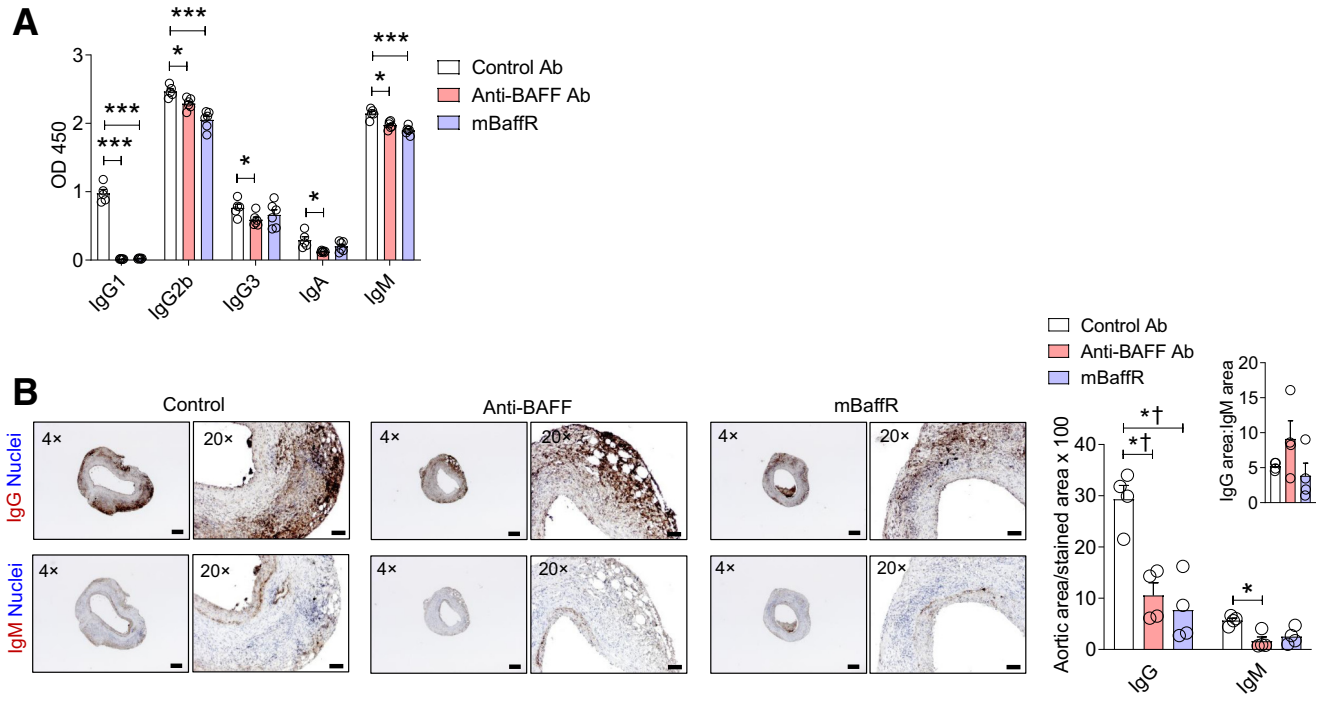

Figure 4 Anti—B-cell-activating factor (BAFF) or mBaffR-mFc (murine BAFF receptor 3 ecto-domain fused to murine IgG1 Fc fragment that blocks binding of BAFF to BAFF receptor 3) treatment has no effect on the aortic IgG:IgM deposition ratio. **A:** Quantification of immunoglobulins in the plasma of the intervention groups. **B:** Representative images and the quantification of IgG and IgM-stained areas in the abdominal aortic aneurysm by using ImageJ. Data are expressed as means ± SEMs. $n = 5$ to 6 (**A**); $n = 4$ mice, 3 sections per mouse (**B**). $^{*}P < 0.05$ and $^{***}P < 0.001$ (one-way analysis of variance followed by a parametric unpaired *t*-test); $^{\dagger}P < 0.05$ (one-way analysis of variance followed by a nonparametric *U*-test). Scale bars: 200 μm (**B**, **left columns**,); 50 μm (**B**, **right columns**). Original magnification: ×4 (**B**, **left columns**); ×20 (**B**, **right columns**). Ab, antibody.

macrophages. To test this hypothesis, BAFF 3-mer— or 60-mer—treated murine splenic B cells (at 100 ng/mL[29]) were cultured with M1 macrophages (differentiated from the bone marrow of BAFF knock-out mice), and the macrophages were tested for the engulfment of CypHer5E-stained apoptotic thymocytes. In place of unpolarized macrophages, M1 were selected because of establishment of a proinflammatory microenvironment in the aorta as early as 3 days after AAA induction[30] and the finding that macrophages are co-localized with inducible nitric oxide synthase, tumor necrosis factor-α, and IL-1β (Figure 5D). Co-culture of B cells with macrophages did not affect the percentages of macrophages that engulfed apoptotic cells (efferocytosis assay was performed for 1 hour). As expected, 1 hour of cytochalasin D treatment significantly attenuated efferocytosis. Interestingly, B cells, independent of BAFF treatment, impaired engulfment efficiency (median fluorescence intensity of CypHer5E in macrophage-gated population) of the macrophages (Figure 6C). This suggests a direct innate role of B cells in macrophage function.

Some of the macrophages are better phagocytes, which engulf and degrade the internalized materials faster, and this may decrease in CypHer5E fluorescence. A two-color strategy[31] was therefore included in the efferocytosis assay that was performed for 30 minutes by using M0 macrophages. The DiI-stained apoptotic cells were labeled with biotin, an efferocytosis assay was performed, and the macrophages were stained with Alexa Flour 647—conjugated streptavidin to identify the partly internalized or surface-attached apoptotic cells. Because the macrophages were not permeabilized, binding of Alexa Flour 647-streptavidin was not expected for completely internalized biotinylated DiI-labeled apoptotic cells. The data suggest that co-culture of B cells with M0 macrophages did not affect the percentages of macrophages that engulfed apoptotic cells; however, B cells, independent of BAFF treatment, impaired engulfment efficiency of the macrophages (median fluorescence intensity of DiI in macrophage-gated populations that are negative for Alexa Flour 647) (Supplemental Figure S4A). Interestingly, the median fluorescence intensity of DiI in macrophages that were stained with Alexa Flour 647 (indicating partly internalized or surface-attached apoptotic cells) was also significantly lower in the macrophages that were co-cultured with B cells (Supplemental Figure S4B). A 30-minute treatment of macrophages with cytochalasin D before the engulfment assay did not affect the percentages of macrophages that engulfed the apoptotic cells. However, the median fluorescence intensity of DiI is significantly attenuated in these macrophages, indicating that a very low number of apoptotic cells were engulfed by the cytochalasin D—treated macrophages. Altogether, these findings suggest that attenuated efferocytosis activity of macrophages in the presence of B cells may be caused by impaired internalization or surface attachment of apoptotic cells.

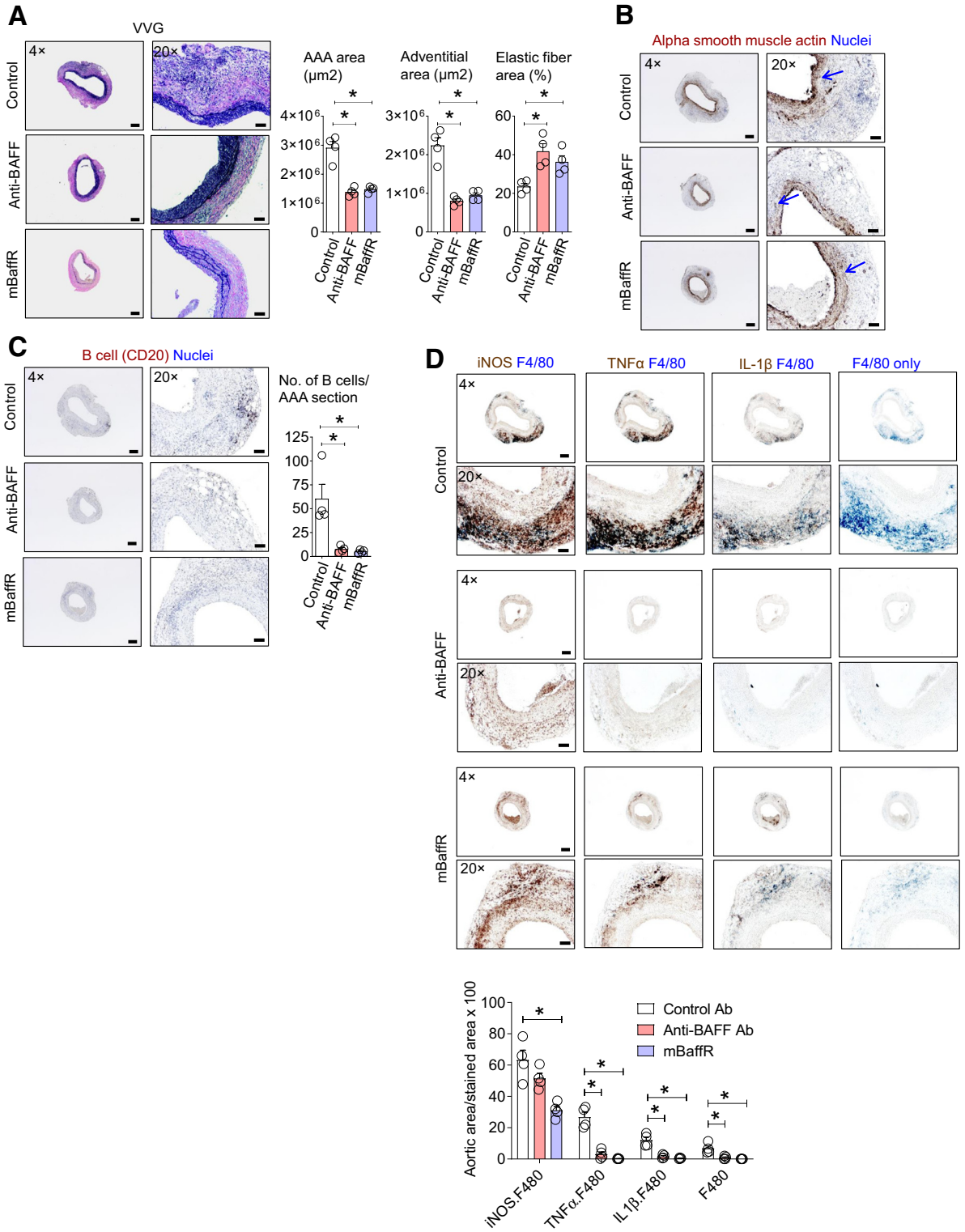

Figure 5 Anti—B-cell-activating factor (BAFF) or mBaffR-mFc (murine BAFF receptor 3 ecto-domain fused to murine IgG1 Fc fragment that blocks binding of BAFF to BAFF receptor 3) treatment attenuates aortic growth and inflammation in abdominal aortic aneurysms (AAAs) of the intervention groups. **A**—**C:** AAA cross-sections of the intervention groups were stained for Verhoeff-Van Gieson (VVG), alpha smooth muscle actin (**arrows** indicate loss of staining), and B cells (anti-CD20 antibody). AAA area, adventitial area, and the elastic fiber area (expressed as percentage of AAA area) were quantified from the VVG-stained sections by using ImageJ. **D:** AAA cross-sections were sequentially stained for inducible nitric oxide synthase (iNOS) and F4/80 (macrophages), tumor necrosis factor-α (TNFα) and F4/80, IL-1β and F4/80, or F4/80 only, and the total stained area was quantified by using ImageJ. Data are expressed as means ± SEM. $n = 4$ mice, 3 to 8 sections per mouse (**A-C**); $n = 4$ mice, 3 sections per mouse (**D**). *$P < 0.05$, determined by one-way analysis of variance followed by a nonparametric *U*-test. Scale bars: 200 μm (**A**, **B**, and **C**, **left columns**, and **D**, **top rows**); 50 μm (**A**, **B**, and **C**, **right columns**, and **D**, **bottom rows**). Original magnification: ×4 (**A**, **B**, and **C**, **left columns**, and **D**, **top rows**); ×20 (**A**, **B**, and **C**, **right columns**, and **D**, **bottom rows**).

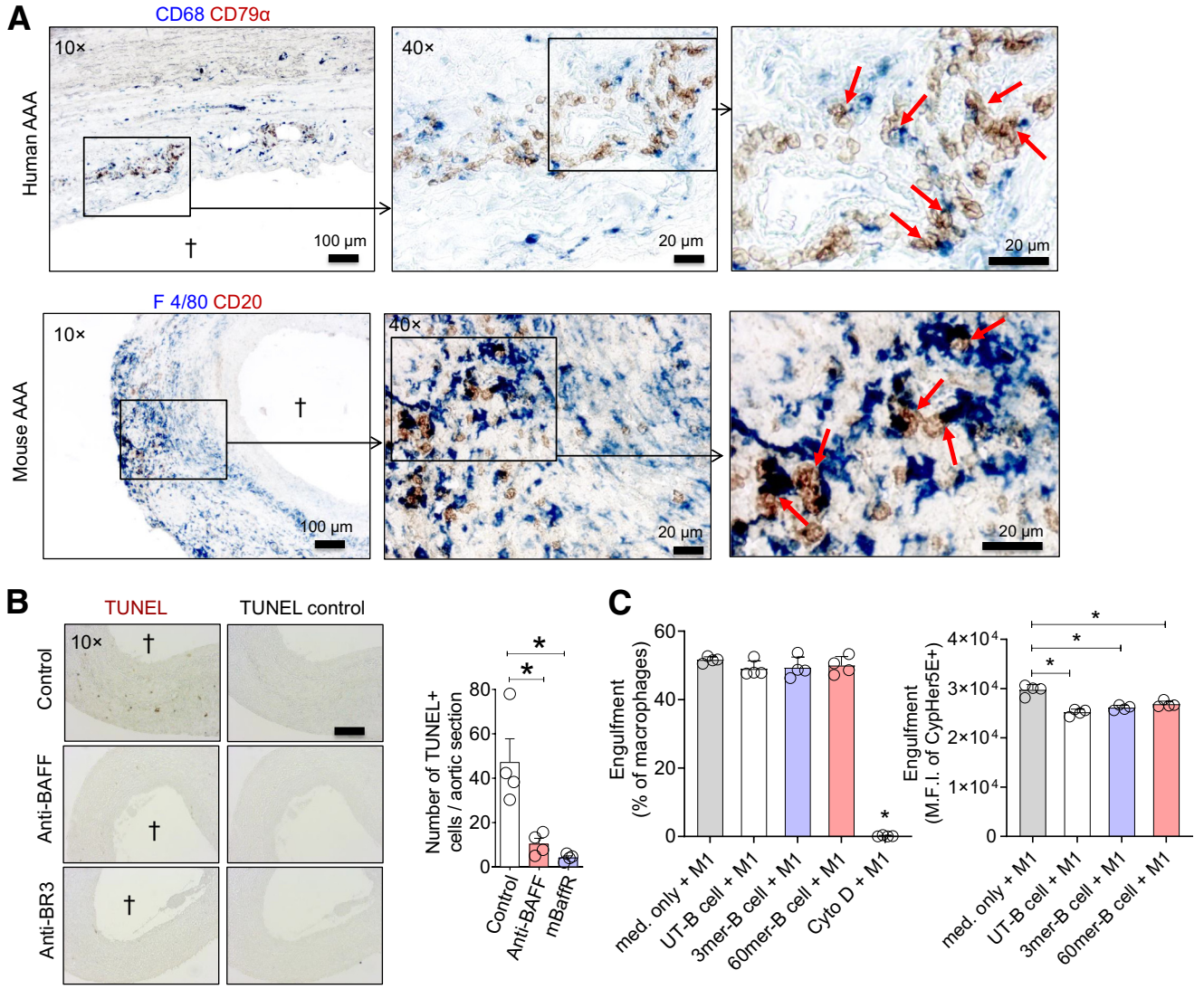

Figure 6 B cells impair efferocytosis activity of macrophages. **A:** Human and mouse abdominal aortic aneurysm (AAA) sections were stained for B cells and macrophages: human AAA, B cells (CD79α, brown) and macrophage (CD68, blue); mouse AAA, B cells (CD20, brown) and macrophages (F4/80, blue). **Arrows** indicate B cells in contact with macrophages in digitally zoomed images. **B:** Terminal deoxynucleotidyl transferase-mediated dUTP nick-end labeling (TUNEL) staining and quantification of the number of TUNEL-positive cells in mouse AAAs. The control sections were not treated with terminal deoxynucleotidyl transferase enzyme. **C:** CytoTracker Green–stained bone marrow–derived macrophages were treated with interferon-γ + lipopolysaccharide to polarize into M1 macrophages and were washed with complete medium to remove interferon-γ and lipopolysaccharide. Purified splenic B cells were left untreated (UT) or treated with 100 ng/mL of B cell–activating factor (BAFF) 3-mer or 60-mer for 16 hours and washed with complete medium to remove BAFF. The M1 macrophages and B cells were co-cultured at 1:1 ratio for 16 hours, and an engulfment assay was performed for 1 hour at 37°C by addition of CypHer5E-stained apoptotic thymocytes. The macrophages were treated for 1 hour with cytochalasin D (Cyto D) (10 μmol/L) before the addition of apoptotic thymocytes as a negative control for the engulfment assay. Flow cytometry was used to determine the engulfment efficiency of the macrophages and to quantify median fluorescence intensity (M.F.I.) of engulfed apoptotic cells. **Daggers** indicate lumen in the AAA sections. Data are expressed as means ± SD (**C**). $n = 4$ mice, 3 sections per mouse (**B**); $n = 4$ (**C**). $^*P < 0.05$, determined by one-way analysis of variance followed by a nonparametric *U*-test. Scale bars: 100 μm (**A**, **left panel**); 20 μm (**A**, **middle** and **right panels**); 200 μm (**B**). Original magnification: ×10 (**A**, **left panel**, and **B**); ×40 (**A**, **middle** and **right panels**).

Discussion

Murine models of AAA, which are known to recapitulate the early stages of human AAA, are used to understand the mechanism of AAA growth. Previously, B cells were identified in human and murine AAAs.[7] Although B cell–deficient muMT mice developed AAA similar to the WT mice,[7] depletion of B cells in WT mice attenuated AAA formation.[8] Some reports suggest a critical role for homeostasis of immune cells in murine experimental AAAs. Here, the critical role of B2 cells in AAA formation was explored by using previously reported B2 cell–depleting activity of BAFF antagonists.[15,18]

B2 cells are the primary B-cell subtype that infiltrates murine AAAs.[8] Differentiation and proliferation of B2 cells or the mature B-cell subsets require soluble BAFF and the

BAFF receptor BR3 on the B-cell surface. Proteolytic cleavage of the membrane-bound BAFF to soluble BAFF 3-mer, which primarily binds to BR3, is critical for survival of B2 cells.[11] Both the human and mouse BAFF share the property of highly active 60-mer formation, which can bind to BAFF receptors BR3, TACI, and BCMA.[13] Immunohistology of AAA tissues shows that B cells are localized in the microenvironment of BAFF. Currently, no techniques are available to detect BAFF 3-mer and 60-mer in the tissue. Presence of B cells expressing BR3, TACI, or BCMA in the AAA tissues suggests that if BAFF 60-mer is present in the AAA tissues, it would strongly activate B cells by binding to BR3 or all multiple BAFF receptors.

Mice genetically deficient in either BAFF or BR3 exhibit a similar immune phenotype, such as: i) lower numbers of mature B cells, ii) a lower number of B2 cells in spleen, iii) lower expression levels of CD21 and CD23 on B cells (B2-cell maturation markers), and iv) reduced antigen-specific Ab response.[32,33] BAFF also increases the expression levels of mature B-cell markers CD21 and CD23 and major histocompatibility complex II on the surface of B cells.[13,34] Here, the BAFF antagonists, anti-BAFF Ab that blocked both the BAFF 3-mer and 60-mer activity, or the mBaffR-mFc that blocked the BAFF activity relayed only via the BR3, attenuated AAA formation. The antagonists not only depleted B2 cells but also the B1 cells and partly depleted plasma IgG2b and IgM levels and deposition of IgG and IgM in AAA in the intervention groups. However, the ratio of deposition of IgG to IgM was found to be similar in the control Ab−treated group and the BAFF antagonist−treated group, suggesting that impaired immunoglobulin levels were not critical for AAA formation in this study. BAFF antagonism significantly depleted B1- and B2-cell populations and, as expected, decreased the surface expression levels of CD23 and major histocompatibility complex II on B cells in the spleen and in circulation. However, because the aortic digestion method depletes some of the markers of the mature B-cell subsets such as CD23,[7] aortic infiltrated B-cell subsets were not identified in this study. Altogether, a short period of treatment of BAFF antagonists (ie, 7 days in the intervention strategy) revealed a significant neutralization of BAFF activity and depletion of B2 cells in mice.

Adaptive immune response against antigens takes weeks to develop; in our study, AAA growth was attenuated when antagonists were injected 7 days after the aneurysm induction. This finding suggests a dominant role of innate immune response in aneurysm formation in the topical elastase model of AAA. In this line, a significant depletion of B cells and proinflammatory macrophages was observed in the AAA tissues of the antagonist-treated mice. In elastase-induced AAAs, despite the fact that B cells comprise only 4% to 5% of the aortic infiltration hematopoietic cells,[7] B-cell depletion attenuates AAA formation.[8] Mellak et al[35] reported that B cells, with the help of exogenously administered human angiotensin II, mobilize splenic monocytes to the aorta to promote AAA formation in apolipoprotein E−deficient mice. However, innate immune response by B cells can modulate the role of highly populated immune cells such as macrophages in AAAs and promote AAA growth. Importantly, adaptive immune cells such as B cells and T cells are known to affect the activity of innate immune cells.[36] Generation of elastin degradation peptides in AAAs polarizes macrophages to the M1 type, which promotes the growth of aortic diameter during AAA formation.[37,38] Here, a significant area of AAAs of the control Ab−treated group was identified with pro-inflammatory or M1 macrophages, whereas AAAs of the anti-BAFF− and mBaffR-mFc−treated groups had negligible macrophage content. Furthermore, a significant number of apoptotic cells were detected in the AAA of the control Ab−treated mice.

These results are suggestive of a dominant role of impaired resolution of inflammation during AAA formation. In support of this *in vivo* observation, our *in vitro* B cell/macrophage co-culture studies show that B cells impair efferocytosis activity of M1 macrophages and unpolarized M0 macrophages. Although a 10% to 15% reduction in the fluorescence intensity of the engulfed apoptotic cells was observed in this study, such a reduction in engulfment can have a profound physiological consequence, as reported previously.[31,39] Moreover, the high number of apoptotic cells observed in AAA tissue (Figure 6B) is a result of accumulation of apoptotic cells at least for 7 days after the administration of control Ab.

This study has a few limitations. In the *in vitro* studies, human recombinant BAFF on murine B cells was used. Murine BAFF may have different effects than human BAFF on murine B cells; however, similar functions of human and murine BAFF are corroborated by the fact that BAFF-deficient mice mimicked the phenotype of WT mice after administration of human BAFF 3-mer.[11] Furthermore, replacing mouse BAFF with human BAFF in a humanized mouse model did not affect B-cell maturation.[40] Apart from mature B cells, BR3 is also expressed on other immune cells such as T cells and macrophages, which are commonly found in murine AAA tissues. Therefore, the possible protective effect of BAFF antagonism on AAA formation could be caused by depletion of both B and other immune cells. However, in a previous study, no significant differences in populations of $CD4^+$ T cells, $CD8^+$ T cells, natural killer cells, and natural killer T cells were found in the spleens of apolipoprotein E knockout mice and apolipoprotein E/BR3 double knockout mice.[17] BAFF 60-mer can regulate the function of murine macrophages; however, a higher concentration (ie, 600 ng/mL), compared with 100 ng/mL for B cells,[29] is required for this activity.[41]

Apart from these limitations, a recent report showed that BAFF neutralization is protective for atherosclerosis.[41] Mechanistically, BAFF 60-mer-TACI signaling in macrophages repressed proatherogenic chemokines production under hypercholesterolemic conditions in apolipoprotein E knockout mice. However, in this study, the anti-BAFF Ab

used was hamster anti-mouse BAFF Ab (clone 10F4). The anti-BAFF Ab clone used in our study was Sandy-2, which is known to bind to the BR3-, TACI-, and BCMA-binding sites on BAFF.[14] Apart from different effects of anti-BAFF Ab clones, this finding also addresses the possibility of different mechanisms of development of atherosclerosis and AAA in apolipoprotein E knockout and WT mice, respectively.

Although the findings on the protective effects of B-cell depletion (using anti-CD20 Ab) of AAA formation is not new, the current study shows the protective effects of BAFF antagonism on AAA formation. Therapies targeting B-cell depletion and BAFF antagonism can have different outcomes on disease pathology, and hence, a dual immunotherapy is proposed.[42] This study provides a detailed description regarding the effect of BAFF antagonists on the dynamics of B-cell subsets and the growth of established AAA in mice. Furthermore, this study is the first to show that B cells can directly modulate macrophage function.

Acknowledgments

We thank the flow cytometry and microscopy core facilities at East Carolina University, the histology core facility at the University of North Carolina, and the flow cytometry, histology, Cardiovascular Research Center histology, and microscopy core facilities at the University of Virginia for assistance; Dr. Mark D. Mannie (East Carolina University) for kindly providing the culture supernatant containing granulocyte colony-stimulating factor; and Biogen for kindly providing the mBaffR-mFc.

Author Contribution

M.D.S. and W.G.M. performed the murine AAA surgery and analyzed data; M.L. conducted histology staining and analyzed data; M.J.J. performed quantification of histology staining; P.S. and C.A.M. helped with B-cell phenotyping, mouse experiments, and preparation of the manuscript; G.R.U., G.A., and N.L. helped with mouse experiments and preparation of the manuscript; and A.K.M. conceived the project, designed and conducted experiments, analyzed data, and wrote the manuscript.

Supplemental Data

Supplemental material for this article can be found at *http://doi.org/10.1016/j.ajpath.2021.08.012*.

References

1. Bown MJ, Sutton AJ, Bell PR, Sayers RD: A meta-analysis of 50 years of ruptured abdominal aortic aneurysm repair. Br J Surg 2002, 89:714−730
2. Ailawadi G, Knipp BS, Lu G, Roelofs KJ, Ford JW, Hannawa KK, Bishop K, Thanaporn P, Henke PK, Stanley JC, Upchurch GR Jr: A nonintrinsic regional basis for increased infrarenal aortic MMP-9 expression and activity. J Vasc Surg 2003, 37:1059−1066
3. Airhart N, Brownstein BH, Cobb JP, Schierding W, Arif B, Ennis TL, Thompson RW, Curci JA: Smooth muscle cells from abdominal aortic aneurysms are unique and can independently and synergistically degrade insoluble elastin. J Vasc Surg 2014, 60:1033−1041. discussion 1041-1042
4. Rowe VL, Stevens SL, Reddick TT, Freeman MB, Donnell R, Carroll RC, Goldman MH: Vascular smooth muscle cell apoptosis in aneurysmal, occlusive, and normal human aortas. J Vasc Surg 2000, 31:567−576
5. Forester ND, Cruickshank SM, Scott DJA, Carding SR: Functional characterization of T cells in abdominal aortic aneurysms. Immunology 2005, 115:262−270
6. Daugherty A, Manning MW, Cassis LA: Angiotensin II promotes atherosclerotic lesions and aneurysms in apolipoprotein E-deficient mice. J Clin Invest 2000, 105:1605−1612
7. Meher AK, Johnston WF, Lu G, Pope NH, Bhamidipati CM, Harmon DB, Su G, Zhao Y, McNamara CA, Upchurch GR Jr, Ailawadi G: B2 cells suppress experimental abdominal aortic aneurysms. Am J Pathol 2014, 184:3130−3141
8. Schaheen B, Downs EA, Serbulea V, Almenara CCP, Spinosa M, Su G, Zhao Y, Srikakulapu P, Butts C, McNamara CA, Leitinger N, Upchurch GR Jr, Meher AK, Ailawadi G: B-cell depletion promotes aortic infiltration of immunosuppressive cells and is protective of experimental aortic aneurysm. Arterioscler Thromb Vasc Biol 2016, 36:2191−2202
9. Moore PA, Belvedere O, Orr A, Pieri K, LaFleur DW, Feng P, Soppet D, Charters M, Gentz R, Parmelee D, Li Y, Galperina O, Giri J, Roschke V, Nardelli B, Carrell J, Sosnovtseva S, Greenfield W, Ruben SM, Olsen HS, Fikes J, Hilbert DM: BLyS: member of the tumor necrosis factor family and B lymphocyte stimulator. Science 1999, 285:260−263
10. Castigli E, Wilson SA, Scott S, Dedeoglu F, Xu S, Lam K-P, Bram RJ, Jabara H, Geha RS: TACI and BAFF-R mediate isotype switching in B cells. J Exp Med 2005, 201:35−39
11. Bossen C, Tardivel A, Willen L, Fletcher CA, Perroud M, Beermann F, Rolink AG, Scott ML, Mackay F, Schneider P: Mutation of the BAFF furin cleavage site impairs B-cell homeostasis and antibody responses. Eur J Immunol 2011, 41:787−797
12. Liu Y, Xu L, Opalka N, Kappler J, Shu HB, Zhang G: Crystal structure of sTALL-1 reveals a virus-like assembly of TNF family ligands. Cell 2002, 108:383−394
13. Bossen C, Cachero TG, Tardivel A, Ingold K, Willen L, Dobles M, Scott ML, Maquelin A, Belnoue E, Siegrist C-A, Chevrier S, Acha-Orbea H, Leung H, Mackay F, Tschopp J, Schneider P: TACI, unlike BAFF-R, is solely activated by oligomeric BAFF and APRIL to support survival of activated B cells and plasmablasts. Blood 2008, 111:1004−1012
14. Kowalczyk-Quintas C, Schuepbach-Mallepell S, Vigolo M, Willen L, Tardivel A, Smulski CR, Zheng TS, Gommerman J, Hess H, Gottenberg J-E, Mackay F, Donzé O, Schneider P: Antibodies that block or activate mouse B cell activating factor of the tumor necrosis factor (TNF) family (BAFF), respectively, induce B cell depletion or B cell hyperplasia. J Biol Chem 2016, 291:19826−19834
15. Kyaw T, Cui P, Tay C, Kanellakis P, Hosseini H, Liu E, Rolink AG, Tipping P, Bobik A, Toh BH: BAFF receptor mAb treatment ameliorates development and progression of atherosclerosis in hyperlipidemic ApoE(-/-) mice. PLoS One 2013, 8:e60430
16. Sage AP, Tsiantoulas D, Baker L, Harrison J, Masters L, Murphy D, Loinard C, Binder CJ, Mallat Z: BAFF receptor deficiency reduces the development of atherosclerosis in mice—brief report. Arterioscler Thromb Vasc Biol 2012, 32:1573−1576
17. Kyaw T, Tay C, Hosseini H, Kanellakis P, Gadowski T, MacKay F, Tipping P, Bobik A, Toh B-H: Depletion of B2 but not B1a B cells in

BAFF receptor-deficient ApoE mice attenuates atherosclerosis by potently ameliorating arterial inflammation. PLoS One 2012, 7: e29371
18. Shen L, Chng MHY, Alonso MN, Yuan R, Winer DA, Engleman EG: B-1a lymphocytes attenuate insulin resistance. Diabetes 2015, 64: 593−603
19. Nakamura Y, Abe M, Kawasaki K, Miyake T, Watanabe T, Yoshida O, Hirooka M, Matsuura B, Hiasa Y: Depletion of B cell-activating factor attenuates hepatic fat accumulation in a murine model of nonalcoholic fatty liver disease. Sci Rep 2019, 9:977
20. Lu G, Su G, Davis JP, Schaheen B, Downs E, Roy RJ, Ailawadi G, Upchurch GR Jr: A novel chronic advanced stage abdominal aortic aneurysm murine model. J Vasc Surg 2017, 66:232−242.e4
21. Guo F, Weih D, Meier E, Weih F: Constitutive alternative NF-kappaB signaling promotes marginal zone B-cell development but disrupts the marginal sinus and induces HEV-like structures in the spleen. Blood 2007, 110:2381−2389
22. Kadl A, Meher AK, Sharma PR, Lee MY, Doran AC, Johnstone SR, Elliott MR, Gruber F, Han J, Chen W, Kensler T, Ravichandran KS, Isakson BE, Wamhoff BR, Leitinger N: Identification of a novel macrophage phenotype that develops in response to atherogenic phospholipids via Nrf2. Circ Res 2010, 107:737−746
23. Spinosa M, Su G, Salmon MD, Lu G, Cullen JM, Fashandi AZ, Hawkins RB, Montgomery W, Meher AK, Conte MS, Sharma AK, Ailawadi G, Upchurch GR Jr: Resolvin D1 decreases abdominal aortic aneurysm formation by inhibiting NETosis in a mouse model. J Vasc Surg 2018, 68:93S−103S
24. Shannon AH, Chordia MD, Spinosa MD, Su G, Ladd Z, Pan D, Upchurch GR Jr, Sharma AK: Single-photon emission computed tomography imaging using formyl peptide receptor 1 ligand can diagnose aortic aneurysms in a mouse model. J Surg Res 2020, 251: 239−247
25. Rosenfeld SM, Perry HM, Gonen A, Prohaska TA, Srikakulapu P, Grewal S, Das D, McSkimming C, Taylor AM, Tsimikas S, Bender TP, Witztum JL, McNamara CA: B-1b cells secrete atheroprotective IgM and attenuate atherosclerosis. Circ Res 2015, 117:e28−e39
26. Upadhye A, Srikakulapu P, Gonen A, Hendrikx S, Perry HM, Nguyen A, McSkimming C, Marshall MA, Garmey JC, Taylor AM, Bender TP, Tsimikas S, Holodick NE, Rothstein TL, Witztum JL, McNamara CA: Diversification and CXCR4-dependent establishment of the bone marrow B-1a cell pool governs atheroprotective IgM production linked to human coronary atherosclerosis. Circ Res 2019, 125:e55−e70
27. Centa M, Jin H, Hofste L, Hellberg S, Busch A, Baumgartner R, Verzaal NJ, Enoksson SL, Matic LP, Boddul SV, Atzler D, Li DY, Sun C, Hansson GK, Ketelhuth DFJ, Hedin U, Wermeling F, Lutgens E, Binder CJ, Maegdesfessel L, Malin SG: Germinal center-derived antibodies promote atherosclerosis plaque size and stability. Circulation 2019, 139:2466−2482
28. Nus M, Sage AP, Lu Y, Masters L, Lam BYH, Newland S, Weller S, Tsiantoulas D, Raffort J, Marcus D, Finigan A, Kitt L, Figg N, Schirmbeck R, Kneilling M, Yeo GSH, Binder CJ, de la Pompa JL, Mallat Z: Marginal zone B cells control the response of follicular helper T cells to a high-cholesterol diet. Nat Med 2017, 23:601−610
29. Smulski CR, Kury P, Seidel LM, Staiger HS, Edinger AK, Willen L, Seidl M, Hess H, Salzer U, Rolink AG, Rizzi M, Schneider P, Eibel H: BAFF- and TACI-dependent processing of BAFFR by ADAM proteases regulates the survival of B cells. Cell Rep 2017, 18: 2189−2202
30. Johnston WF, Salmon M, Su G, Lu G, Stone ML, Zhao Y, Owens GK, Upchurch GR Jr, Ailawadi G: Genetic and pharmacologic disruption of interleukin-1[beta] signaling inhibits experimental aortic aneurysm formation. Arterioscler Thromb Vasc Biol 2013, 33: 294−304
31. Wang Y, Subramanian M, Yurdagul A Jr, Barbosa-Lorenzi VC, Cai B, de Juan-Sanz J, Ryan TA, Nomura M, Maxfield FR, Tabas I: Mitochondrial fission promotes the continued clearance of apoptotic cells by macrophages. Cell 2017, 171:331−345.e22
32. Sasaki Y, Casola S, Kutok JL, Rajewsky K, Schmidt-Supprian M: TNF family member B cell-activating factor (BAFF) receptor-dependent and -independent roles for BAFF in B cell physiology. J Immunol 2004, 173:2245−2252
33. Schiemann B, Gommerman JL, Vora K, Cachero TG, Shulga-Morskaya S, Dobles M, Frew E, Scott ML: An essential role for BAFF in the normal development of B cells through a BCMA-independent pathway. Science 2001, 293:2111−2114
34. Gorelik L, Cutler AH, Thill G, Miklasz SD, Shea DE, Ambrose C, Bixler SA, Su L, Scott ML, Kalled SL: Cutting edge: BAFF regulates CD21/35 and CD23 expression independent of its B cell survival function. J Immunol 2004, 172:762−766
35. Mellak S, Ait-Oufella H, Esposito B, Loyer X, Poirier M, Tedder TF, Tedgui A, Mallat Z, Potteaux S: Angiotensin II mobilizes spleen monocytes to promote the development of abdominal aortic aneurysm in Apoe-/- mice. Arterioscler Thromb Vasc Biol 2015, 35:378−388
36. Kim KD, Zhao J, Auh S, Yang X, Du P, Tang H, Fu Y-X: Adaptive immune cells temper initial innate responses. Nat Med 2007, 13: 1248−1252
37. Dale MA, Xiong W, Carson JS, Suh MK, Karpisek AD, Meisinger TM, Casale GP, Baxter BT: Elastin-derived peptides promote abdominal aortic aneurysm formation by modulating M1/M2 macrophage polarization. J Immunol 2016, 196:4536−4543
38. Batra R, Suh MK, Carson JS, Dale MA, Meisinger TM, Fitzgerald M, Opperman PJ, Luo J, Pipinos II, Xiong W, Baxter BT: IL-1[beta] (Interleukin-1[beta]) and TNF-[alpha] (tumor necrosis factor-[alpha]) impact abdominal aortic aneurysm formation by differential effects on macrophage polarization. Arterioscler Thromb Vasc Biol 2018, 38: 457−463
39. Elliott MR, Zheng S, Park D, Woodson RI, Reardon MA, Juncadella IJ, Kinchen JM, Zhang J, Lysiak JJ, Ravichandran KS: Unexpected requirement for ELMO1 in clearance of apoptotic germ cells in vivo. Nature 2010, 467:333−337
40. Lang J, Zhang B, Kelly M, Peterson JN, Barbee J, Freed BM, Di Santo JP, Matsuda JL, Torres RM, Pelanda R: Replacing mouse BAFF with human BAFF does not improve B-cell maturation in hematopoietic humanized mice. Blood Adv 2017, 1:2729−2741
41. Tsiantoulas D, Sage AP, Göderle L, Ozsvar-Kozma M, Murphy D, Porsch F, Pasterkamp G, Menche J, Schneider P, Mallat Z, Binder CJ: B cell-activating factor neutralization aggravates atherosclerosis. Circulation 2018, 138:2263−2273
42. Lin WY, Seshasayee D, Lee WP, Caplazi P, McVay S, Suto E, Nguyen A, Lin Z, Sun Y, DeForge L, Balazs M, Martin F, Zarrin AA: Dual B cell immunotherapy is superior to individual anti-CD20 depletion or BAFF blockade in murine models of spontaneous or accelerated lupus. Arthritis Rheumatol 2015, 67:215−224